Taylor & Francis
Taylor & Francis Group

RESEARCH PAPER

Cholix protein domain I functions as a carrier element for efficient apical to basal epithelial transcytosis

Alistair Taverner [a], Julia MacKay[a], Floriane Laurent[a], Tom Hunter[b], Keyi Liu[b], Khushdeep Mangat[b], Lisa Song[b], Elbert Seto[b], Sally Postlethwaite[b], Aatif Alam[b], Apurva Chandalia[b], Minji Seung[b], Mazi Saberi[b], Weijun Feng[b], and Randall J. Mrsny [a,b]

aDepartment of Pharmacy and Pharmacology, University of Bath, Bath, England; bApplied Molecular Transport, South San Francisco, CA, USA

ABSTRACT

Cholix (Chx) is expressed by the intestinal pathogen *Vibrio cholerae* as a single chain of 634 amino acids (~70.7 kDa protein) that folds into three distinct domains, with elements of the second and third domains being involved in accessing the cytoplasm of nonpolarized cells and inciting cell death via ADP-ribosylation of elongation factor 2, respectively. In order to reach nonpolarized cells within the intestinal lamina propria, however, Chx must cross the polarized epithelial barrier in an intact form. Here, we provide *in vitro* and *in vivo* demonstrations that a nontoxic Chx transports across intestinal epithelium via a vesicular trafficking pathway that rapidly achieves vesicular apical to basal (A→B) transcytosis and avoids routing to lysosomes. Specifically, Chx traffics in apical endocytic Rab7$^+$ vesicles and in basal exocytic Rab11$^+$ vesicles with a transition between these domains occurring in the ER-Golgi intermediate compartment (ERGIC) through interactions with the lectin mannose-binding protein 1 (LMAN1) protein that undergoes an intracellular re-distribution that coincides with the re-organization of COPI$^+$ and COPII$^+$ vesicular structures. Truncation studies demonstrated that domain I of Chx alone was sufficient to efficiently complete A→B transcytosis and capable of ferrying genetically conjoined human growth hormone (hGH). These studies provide evidence for a pathophysiological strategy where native Chx exotoxin secreted in the intestinal lumen by nonpandemic *V. cholerae* can reach nonpolarized cells within the lamina propria in an intact form by using a nondestructive pathway to cross in the intestinal epithelial that appears useful for oral delivery of biopharmaceuticals.

One-Sentence Summary: Elements within the first domain of the Cholix exotoxin protein are essential and sufficient for the apical to basal transcytosis of this *Vibrio cholerae*-derived virulence factor across polarized intestinal epithelial cells.

Introduction

The intestinal mucosa establishes and maintains a critical barrier to the casual uptake of macromolecular materials that enter through diet and that are produced by resident elements of the microbiome. A delicate, single layer of columnar epithelial cells joined by tight junctions function to selectively regulate the movement of solutes and ions to produce a highly effective, yet remarkably dynamic barrier.[1] The intercellular tight junctional complexes restrict the movement of potential therapeutic agents with a molecular mass of greater than ~500 Da between adjacent epithelial cells; the so-called paracellular route. Thus, macromolecules that cannot travel through the paracellular route may be absorbed at the luminal surface of the epithelium through receptor- and/or fluid phase-mediated uptake mechanisms, but their fate typically involves recycling back into the lumen and/or routing to the lysosomal degradation pathway.[2] Intestinal epithelial homeostasis involves interactions with a plethora of bacteria, fungi, and viruses that comprise the microbiome residing at the luminal surface,[3] and these microbes secrete a variety of virulence factors that function to modulate the properties and functions of the intestinal barrier. While symbiotic interactions occurring between commensal bacteria and the underlying host tissue are beneficial for health, it is well established that pathogen-driven dysbiosis can occur in this environment that engages rectifying immune responses.[4]

One strategy used by pathogens to stabilize luminal infections involves secretion of virulence factors capable of limiting the immunological response by targeted destruction of antigen presentation and/or immunological effector cells positioned in the *lamina propria* compartment that exists just beneath the epithelium.[5] *Vibrio cholerae* is an intestinal pathogen that is best known for its induction of a watery diarrhea induced by the actions of cholera toxin (CTx) during pandemic infections that flush these bacteria from the intestine to provide a mechanism for pathogen dissemination to additional hosts.[6] There are, however, nonpandemic variants of *V. cholerae* that do not express CTx and instead establish a more durable infection within the intestinal lumen.[7] Such *V. cholerae* infections are associated with virulence factors other than CTx,[8,9] proving a potential basis for stable intestinal infections of nonpandemic strains;[10] one such virulence factor is cholix.[11]

Cholix (Chx) is composed of a single chain of 643 amino acids that folds into domains designated as Ia, II, Ib, and III; this order reflects its folded organization with relation to its N- to C-terminus orientation.[11] Chx can intoxicate nonpolarized cells through a mechanism that involves several steps: 1) receptor-mediated endocytosis, 2) furin cleavage at position R^{292}, 3) retrograde vesicular trafficking to the endoplasmic reticulum (ER) facilitated by a C-terminal KDEL amino acid sequence, and 4) transfer of amino acids 293–643 to the cell cytoplasm through a mechanism that may involve the Sec61 translocon.[12] These steps are considered essential to the presumed virulence function of Chx that involves cytoplasmic delivery of an enzymatic activity within domain III of the protein that ADP-ribosylates cytoplasmic elongation factor 2 to suppress protein synthesis to induce apoptosis. To date, Chx structure/function studies have focused on how this exotoxin intoxicates nonpolarized cells such as those that would be present in the *lamina propria* of the intestinal mucosa as a way to stabilize nonpandemic *V. cholerae* in the intestinal lumen.[11,13] At present, the mechanism(s) by which Chx can reach these cells following secretion from luminal *V. cholerae* is unclear. Herein, we present several key findings related to the apical to basal (A→B) transcytosis mechanism used by Chx to reach nonpolarized cells within the *lamina propria*.

While some bacterial exotoxins are capable of damaging the intestinal barrier to gain systemic access for the pathogen,[14] we would predict this strategy would be incompatible with maintaining a chronic, nonpandemic *V. cholerae* infection at the intestinal luminal surface.[10] We hypothesized that Chx must transport across intact polarized intestinal epithelia without significant epithelial damage and should avoid enzymatic and/or lysosomal environments during this transport that could destroy its capacity to reach the *lamina propria* in a functional form. A few bacterial exotoxins are known to use mechanisms that avoid such a destructive fate in nonpolarized cells,[15] however, there have been only limited studies describing their transport in polarized epithelial cells.[16] Here, we examined the possibility that Chx utilizes a pathway through polarized intestinal epithelial cells to achieve efficient apical to basal (A→B) transcytosis in order to reach *lamina propria* cell populations for delivery of its toxic payload.

We now demonstrate that a nontoxic form of full-length Chx (ntChx) can rapidly and efficiently transport across human intestinal epithelia *in vitro* and rat jejunum *in vivo* and that truncations of Chx showed that domain I was sufficient for A→B transcytosis. Consistent with our hypothesis, Chx appears to avoid the lysosomal degradation pathway in polarized intestinal epithelial cells. Following apical entry, Chx appears in a vesicular compartment associated with early endosomes, but avoids the default trafficking pathway to lysosomes. Chx A→B transcytosis is associated with a re-distribution of $COPI^+$ and $COPII^+$ vesicles and movement of LMAN1 (lectin mannose-binding protein 1) protein from an apical only to an apical and basal vesicular compartment distribution. Once in the basal vesicular compartment, Chx appears to engage recycling endosomal structures as part of an exocytosis strategy to enter the *lamina propria*. Overall, our data support a role for Chx domain I to facilitate efficient A→B transcytosis across intact, polarized epithelia to deliver this protein to nonpolarized cells within the *lamina propria* that could then be intoxicated to aid in stabilizing luminal infections of nonpandemic *V. cholerae*. Using this information, we demonstrated the capacity of Chx domain I to ferry biologically active human growth hormone (hGH) across intestinal epithelium *in vivo* as

a proof-of-concept to demonstrate the potential use of this A→B transcytosis pathway for the efficient oral delivery of protein therapeutics.

Results

In vitro Chx A→B transport across the intestinal epithelium does not involve cell intoxication

In order to test the hypothesis that Chx intoxication of epithelial cells is not required for efficient apical to basal (A→B) transport of this toxin from the intestinal lumen to reach nonpolarized target cells within the *lamina propria*, we examined the capacity of a nontoxic form of Chx to undergo A→B transport. Mutation of a single glutamic acid to alanine, $E^{581}A$, within the enzymatic pocket of Chx domain III ablates the intoxicating ADP-ribosylation function of this protein.[11] Further, a free cysteine residue was placed at the C-terminus of the ntPE protein that was used to specifically attach a biotin residue (Figure 1a). A→B transport at 37°C of biotin-labeled, nontoxic Chx^{E581A} (ntChx) was measured across confluent sheets of primary human intestinal epithelium *in vitro*, with concentrations of 2.5–200 µg/mL being applied to the apical surface and the amount of ntChx-biotin in the basal compartment being measured by ELISA after 2 h (Figure 1b). This concentration range demonstrated an apparent permeability (P_{aap}) for apical ntChx-biotin concentrations of 2.5–20 µg/mL that was roughly two-fold greater than for apical concentrations above 20 µg/mL, although all concentrations showing remarkable efficiencies for transport of this ~70 kDa protein. This change in permeability rates is consistent with a receptor-mediated transport mechanism that saturated at ~20 µg/mL for the 0.6 cm^2 filter surface area systems of the primary human intestinal epithelium used for this *in vitro* study. Importantly, transported biotin-labeled ntChx was not strikingly modified in its apparent size by this transcytosis event as assessed by Western blot analysis, suggesting a lack of extensive degradation or modification (Figure 1c). During the 2-h time course of these transcytosis studies, the transepithelial electrical resistance (TEER) remained at ~300 Ω•cm^2, suggesting that ntChx transport was not due to leakage through the paracellular route (data not shown).

A time-course assessing A→B transport following the apical application of 5, 10, and 20 µg/mL ntChx-biotin demonstrated linearity after a lag phase of ~20–25 min (Figure 1d). The P_{aap} of ntChx-biotin at 37°C was calculated to be ~1.92 x 10^{-5} cm/s, with apical concentration of ntChx-biotin becoming limited after ~90 min in this *in vitro* model. Permeability of ntChx-biotin was dramatically reduced when the same transport protocol was performed at 4°C (Figure 1d), supporting the concept that ntChx transport involved an energy-dependent transcytosis mechanism. Together, these data suggest that A→B transport of ntChx involves a highly efficient, active transport process that delivers intact ntChx to the basal compartment, suggesting that the pathway accessed by this exotoxin was privileged from significant catabolism or modification. Cholix cleavage at position R^{293} by the serine protease furin is required for activation of the toxin as part of its intoxication mechanism.[11] This cleavage event separates the C-terminal toxic domain from the N-terminal segment of the protein, presumably occurring in an acidified vesicular compartment following endocytosis in nonpolarized cells. Since the ntChx transported across polarized intestinal epithelial cells *in vitro* appeared to maintain its full-length size of ~70.7 kDa, we examined whether the ntChx used in these transcytosis studies could be cleaved as anticipated. Exposure to the serine protease trypsin separated ntChx at pH 6, but not at pH 7.4 (Figure 1e). As a control, bovine serum albumin was similarly exposed to trypsin at these two pH conditions. These results showed that the ntChx used in these transcytosis studies was capable of selective, pH-dependent serine-protease cleavage as might be expected to occur in nonpolarized cells as part of the intoxication mechanism for Chx-mediated killing of nonpolarized cells.

The apical membrane surface pH of the small intestinal epithelium has been suggested to be between 5 and 7.[17] A→B transport across primary human intestinal epithelium *in vitro* was observed to be approximately twice as efficient when the apical media was pH 7 compared to pH 5, while the basal pH of 7 or 5 did not have an effect (Figure 1f). The greater variability observed for outcomes where the apical pH of 5 was tested on ntChx transport may have been due to partial neutralization of the apical compartment during the course of the study. In sum, these data suggest that ntChx is capable of efficient, consistent, and continuous transport across the human intestinal epithelium through a process that
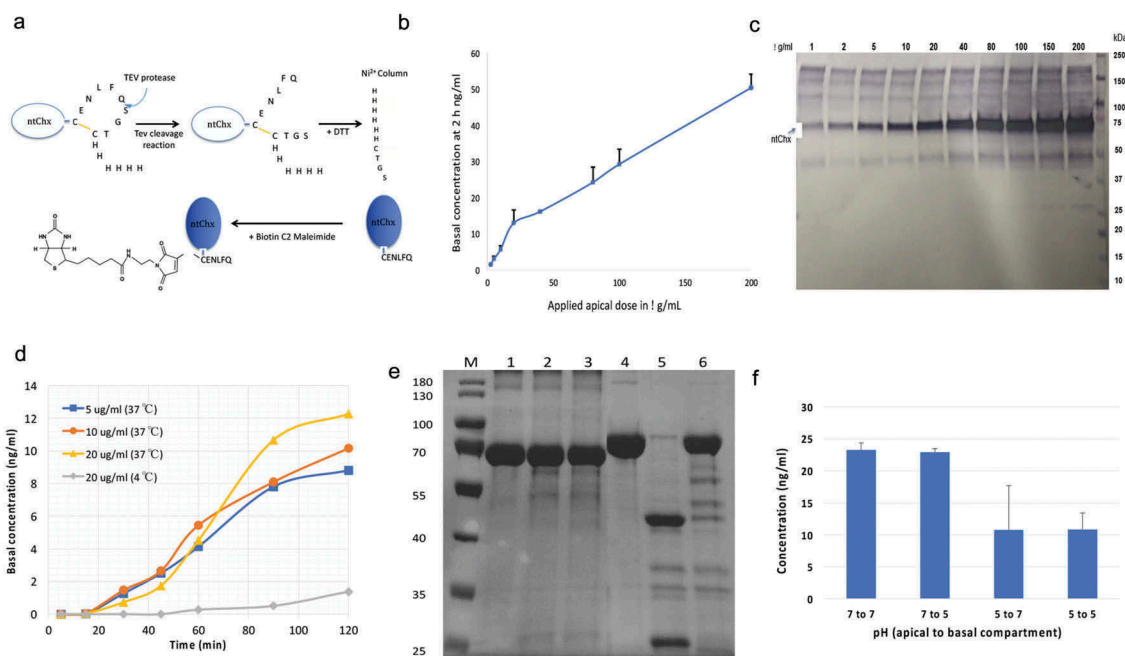
Figure 1. Nontoxic cholix (ntChx) can undergo apical to basal (A➤B) transport across human polarized intestinal epithelium *in vitro*. (a) A C-terminal disulfide constrained loop containing a tobacco etch virus (TEV) protease-specific sequence followed by a hexa-histidine sequence, introduced genetically at the C-terminus of ntChx, was used to generate properly folded ntChx with a single free sulfhydryl moiety that could be selectively conjugation to maleimide-biotin. (b) Amount of ntChx-biotin detected in basal compartment 2 h after apical application of 2.5–200 mg/mL (N = 3; mean ± SE). (c) Basal compartment contents 2 h after apical application of 2.5–200 mg/mL ntChx-biotin that were concentrated approximately 10-fold prior to Western blot analysis. (d) Basal quantities of ntChx-biotin over a time course of 2 h following apical application of 5–20 mg/mL at 37℃ or 4℃. (e) Trypsin cleavage of ntChx *in vitro*. M = molecular weight standards; 1 = undigested bovine serum albumin (BSA); 2 = BSA digest at pH 6; 3 = BSA digest at pH 7.4; 4 = undigested ntChx; 5 = ntChx digest at pH 6; 6 = ntChx digest at pH7.4. (f) A➤B transport of 20 mg/mL ntChx-biotin after 120 min where the apical and basal compartment pH was initially at either 7 or pH 5 (N = 2; mean ± SE). Data shown in (b), (d), and (f) were collected using an ELISA that captured biotin-labeled ntChx with streptavidin and detected with anti-ntChx polyclonal antibody.

does not result in significant size modification to the transported protein.

In vivo A→B transcytosis across rat intestinal epithelium

We next examined the fate of ntChx applied to the apical surface of rat jejunum by direct intra-luminal injection (ILI) *in vivo*; consistent *in vitro* studies (Figure 1), ntChx transport was completed within 15 min with no involvement of the paracellular route (Figure 2). Further, ntChx remained within vesicular structures and failed to access the cytoplasm of polarized epithelial cells, unlike its fate in nonpolarized cells within the *lamina propria*, consistent with vesicular trafficking that was distinct from events associated with toxin trafficking in nonpolarized cells.[18,19]

Chx can enter nonpolarized cells using a clathrin-dependent endocytosis mechanism involving the low-density lipoprotein receptor-related protein, but may also utilize additional cell-entry mechanisms.[11] Besides endocytosis processes, clathrin also functions in selective cargo sorting at the *trans*-Golgi network (TGN).[20] Co-localization of ntChx with clathrin was observed extensively within the apical and basal vesicular compartments of enterocytes, but not at the apical plasma membrane and not in the supranuclear area of enterocytes (Figure 2a). This suggested that ntChx/clathrin co-localizations were not associated with apical endocytosis or TGN sorting, but possibly in endosomes involved in cellular trafficking in the apical and basal compartments.[21] Thus, ntChx appears to use a clathrin-independent endocytosis process but clathrin-dependent trafficking mechanism(s) during A→B transcytosis.

Upon endocytosis, ntChx was observed to co-localize with early endosomal antigen 1 (EEA1) in the apical compartment within enterocytes near the
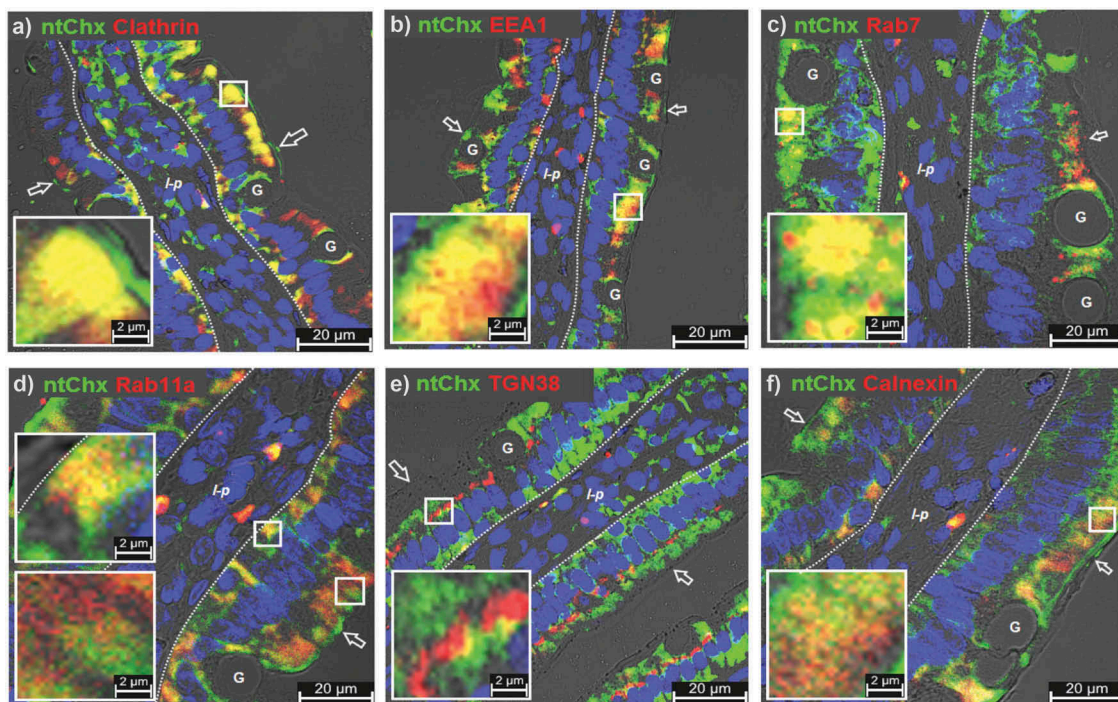
Figure 2. Nontoxic cholix (ntChx) undergoing A→B transcytosis *in vivo* co-localizes with discrete vesicular compartments. Immunofluorescence microscopy was performed on rat jejunum at 15 min after intraluminal injection. Co-localization of ntChx and (a) clathrin or (b) early endosomal antigen-1 (EEA-1) or (c) late endosome marker Rab7 or (d) recycling endosome marker Rab11a or (e) *trans*-Golgi network 38 protein (TGN-38) or (f) calnexin is shown. Arrow = apical (luminal) epithelial membrane; dashed line = epithelial cell-basement membrane demarcation; *l-p* = lamina propria G = goblet cell. Nuclei stained with 4′,6-diamidino-2-phenylindole (DAPI; blue).

apical plasma membrane (Figure 2b), supporting the idea that this exotoxin enters into intestinal epithelial cells through a receptor-mediated endocytosis [22] Co-localizations observed between ntChx and EEA1 at 15 min were primarily restricted to an apical enterocyte compartment, with limited co-localization events between ntChx and EEA1 being observed in the basal compartment of enterocytes. Some of the apical vesicular structures containing ntChx were also positive for Rab7 (Figure 2c), a protein involved in early-to-late endosome maturation, modulation of ER homeostasis and stress, and endosome-to-TGN trafficking.[23–25] Similar to EEA1, Rab7/ntChx co-localizations were restricted to the apical region of enterocytes, with large Rab7+ vesicles being present that were consistent with lysosomal structure but which did not contain ntChx.

Rab11a, known to be associated with recycling endosomes,[22] was observed in both apical and basal compartments of enterocytes but co-localization with ntChx-containing vesicles, interestingly, was limited to the basal compartment (Figure 2d). Recycling endosomes can intersect with the TGN

as part of its secretory pathway sorting function to direct newly synthesized proteins to various locations in the cell.[23] Notably, ntChx co-localized with TGN38, a protein indicative of the TGN, in a discrete band of vesicles in the supranuclear region of enterocytes; ntChx/TGN38 co-localization events in nonpolarized cells within the *lamina propria* following enterocyte transcytosis were limited (Figure 2e). Calnexin, an ER-located lectin chaperone involved in regulating the free cytosolic Ca^{2+} concentration,[26] showed limited co-localizations with ntChx in the apical compartment of enterocytes (Figure 2f). Together, these co-localization studies demonstrated that ntChx efficiently enters at the apical plasma membrane of enterocytes and associates with vesicular structures that define a discrete set of trafficking pathway events. A→B transcytosis of ntChx appeared to also occur efficiently through goblet cells but visualization of the intracellular distribution of ntChx within these cells was not as clear as in enterocytes due to the presence of the large numbers (and volume) of secretory vesicles containing mucus.

Cholix domain I is sufficient for A→B transcytosis in vivo

We next tested the hypothesis that elements within Chx domain I are sufficient to ferry the cytoplasmic accessing function and toxic payload elements of this protein present in domains II and III across polarized epithelial cells to reach and intoxicate nonpolarized cells within the *lamina propria*. Previously, *in vivo* A→B transcytosis was monitored by immunofluorescence microscopy using a polyclonal antibody raised against the full-length ntChx protein. Since it was unclear if the polyclonal antibody raised to full-length ntChx would adequately recognize Chx domain I, we prepared reagents that could be monitored equivalently. Genetic chimeras of full-length ntChx or Chx domain I, terminating at position K^{266} (Chx266), were prepared where their C-termini were genetically conjoined to the N-terminus of red fluorescent protein (RFP). RFP alone, having a molecular weight of 25.9 kDa[27] was used as a transcytosis control. No RFP was detected undergoing A→B transcytosis when examined 30 min after ILI into rat jejunum *in vivo* (Figure 3a). Epithelial transcytosis patterns were similar and the extent of RFP detectable in the *lamina propria* was also comparable for both ntChx-RFP (Figure 3b) and Chx266-RFP (Figure 3c). Notably, the extent of RFP detected in the *lamina propria* was extensively associated with most cells in the compartment and comparable for ntChx-RFP and Chx266-RFP. These results suggest that elements within Chx required for A→B transcytosis reside within domain I and that this domain was sufficient to ferry a protein cargo across the intestinal epithelium *in vivo*. Further, domain I appears to provide comparable targeting to cells with the *lamina propria* as full-length Chx.

Cholix domain I is directed away from lysosomes during A→B transcytosis in vivo

The remarkable efficiency of ntChx-mediated A→B transcytosis suggests that the default mechanism of lysosomal destruction for nonspecific uptake of proteins following endocytosis at the luminal intestinal surface is somehow avoided.[17] To examine this point, we first followed the fate of hGH administered by ILI into rat jejunum epithelial cells *in vivo*. Immunofluorescence detection of hGH was limited to a small population of vesicles in the apical region of enterocytes following nonspecific fluid-phase uptake and with no evidence of A→B transcytosis (Figure 4a). By 15 min post-ILI, hGH was observed to co-localize with Lamp1 (Figure 4b, **line-intensity profile plot**) and Rab7 (Figure 4c) with about the same frequency and characteristics of resident Lamp1$^+$, Rab7$^+$ vesicles that would be consistent with lysosomes present in these cells (Figure 4d). Similar co-localizations between Chx266-hGH and Lamp1 (Figure 4e, **line-intensity profile plot**) or Rab7 (Figure 4f) did not occur for this chimera during A→B transcytosis. These results suggest that materials covalently associated with Chx can avoid a potential degradative fate that would normally result following fluid-phase endocytosis.[28]
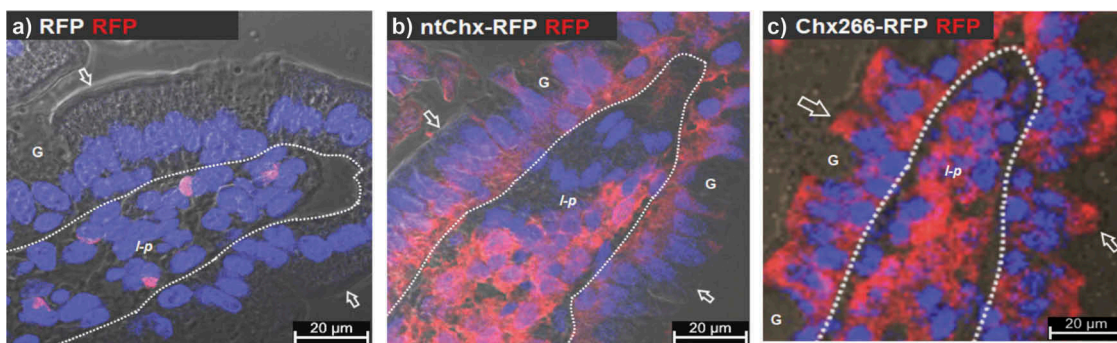

Figure 3. Cholix domain I is sufficient for A→B transcytosis. Immunofluorescence microscopy was performed on rat jejunum at 30-min after intraluminal injection of (a) red fluorescent protein (RFP) or (b) ntChx genetically conjoined to RFP (ntChx-RFP) or (c) cholix truncated amino acid 266 (domain I) and conjoined to RFP (Chx266-RFP). Arrow = luminal (apical) epithelial membrane; dashed line = epithelial cell-basement membrane demarcation; G = goblet cell; *l-p = lamina propria*. Nuclei stained with 4′,6-diamidino-2-phenylindole (DAPI; blue).

Taverner et al   Cholix domain I for oral protein delivery
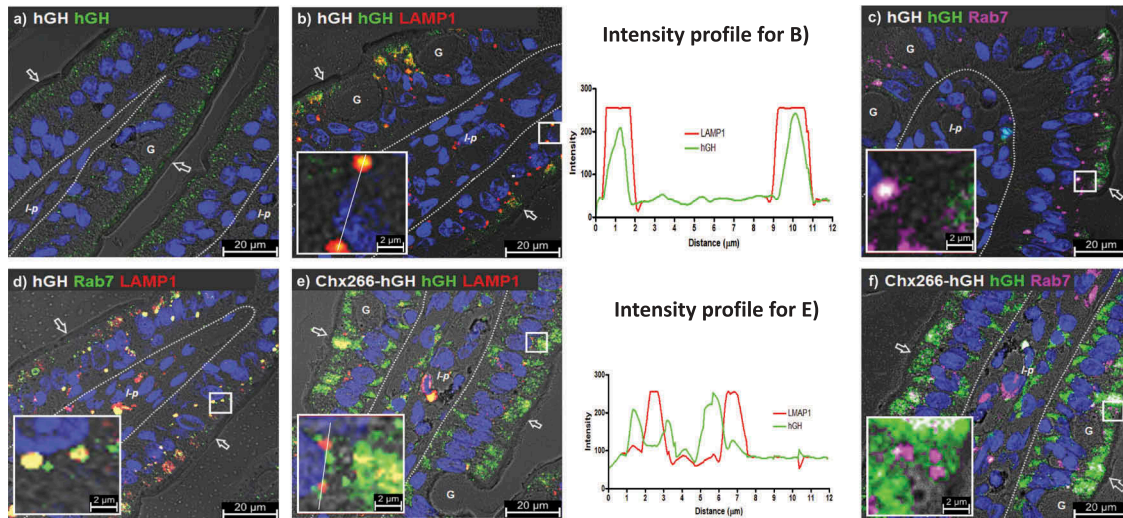
Figure 4. A→B transcytosis of Chx domain I eludes uptake into lysosome-like structures after apical entry into enterocytes following intraluminal infection (ILI) *in vivo*. Immunofluorescence detection at 15-min post-ILI of (a) hGH showed that following fluid-phase uptake of this protein into the apical region of enterocytes it co-localizes with (b **and line-intensity profile plot**) Lamp1 and (c) Rab7 with characteristics consistent with (d) co-localization of Lamp1 and Rab7 at lysosomes. Chx266-hGH co-localization with (e and line-intensity profile plot) LAMP1 or (f) Rab7 was not observed in lysosome-like structures. Arrow = apical epithelial surface; dashed line = epithelial cell-basement membrane demarcation; G = goblet cell; l-p = lamina propria. Nuclei stained with 4',6-diamidino-2-phenylindole (DAPI; blue).

COPI and COPII distribution is affected by Chx trafficking

COPI and COPII coating machineries can be used as hallmarks for the movement of vesicles between the endoplasmic reticulum (ER), ER exit sites, ER-to-Golgi intermediate compartment (ERGIC), Golgi complex, and TGN that provide routing for newly synthesized secretory proteins destined to the secretory and endolysosomal systems as well as directing the fate of internalized proteins following endocytosis at the plasma membrane.[21] In untreated intestinal tissues, COPI was observed to be adjacent to the apical plasma membrane and distributed in the apical vesicular region of rat enterocytes (Figure 5a). Remarkably, by 15 min post-ILI of Chx266-hGH, COPI was observed almost exclusively in the supranuclear region of enterocytes (Figure 5b). A striking re-organization for COPII was also observed: COPII was localized primarily to a supranuclear region and in the basal vesicular region of untreated enterocytes (Figure 5c) but moved to a predominantly apical vesicular region distribution with a much reduced distribution in the basal vesicular region by 15-min post-ILI of Chx266-hGH (Figure 5d). These results suggested that Chx transcytosis coincided with

striking reorganizations of COPI and COPII distribution enterocytes. ILI of hGH alone (not conjoined to Chx266) did not affect COPI or COPII cellular distribution (data not shown).

The extent of COPI and COPII co-localization on individual vesicles was minimal in untreated rat enterocytes (Figure 6a **and line-intensity profile plot**), consistent with their counter-directional vesicle trafficking roles.[21] This limited extent of COPI/COPII co-localization was retained even after their re-organization induced by Chx266-hGH, with these limited co-localizations being observed in the supranuclear region of enterocytes (Figure 6b **and line-intensity profile plot**). Thus, Chx transcytosis induced an exchange of COPI and COPII intracellular distributions for the apical and basal vesicular compartments of enterocytes in a manner that maintained the limited co-localization of these coat proteins in the same vesicle. We next asked whether Chx was present in these re-organized COPI+ and/or COPII+ vesicles over a time course of 5 and 15-min post-ILI. At 5 min, Chx266-hGH showed significant co-localization with COPI in the supranuclear region (Figure 6c **and line-intensity profile plot**), but the extent of this co-localization was reduced by 15 min
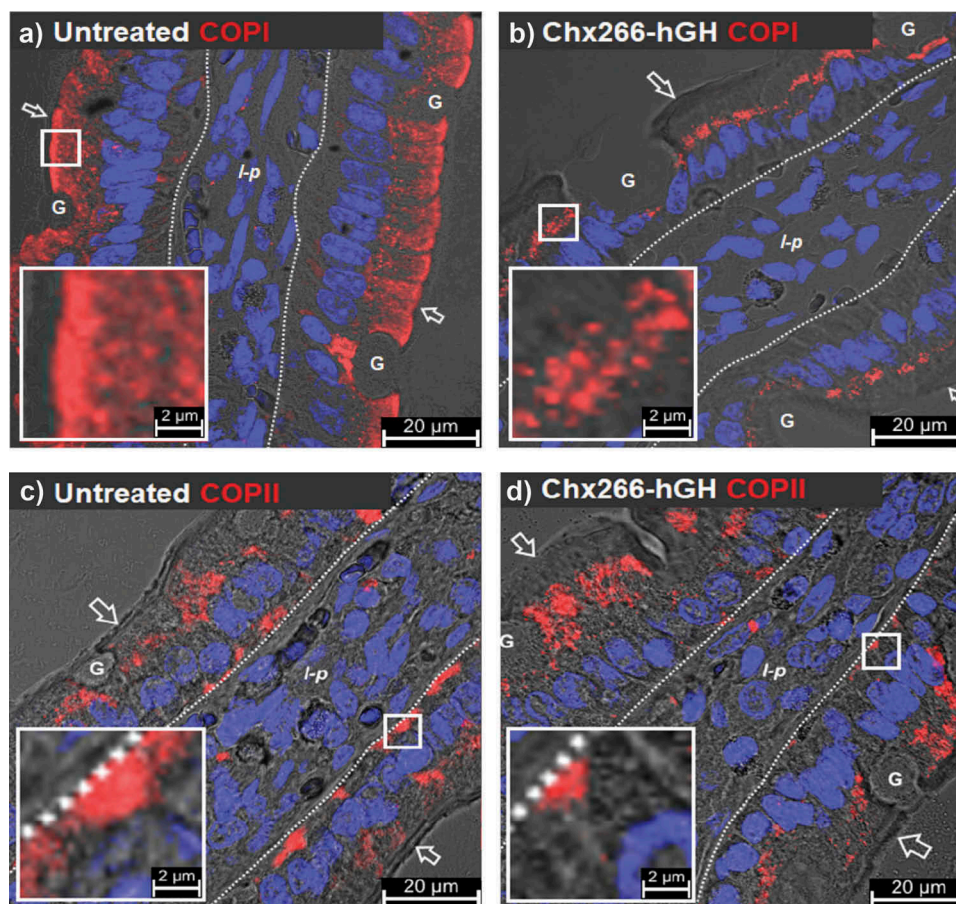
Figure 5. A→B transcytosis of Chx domain I induces a redistribution of COPI and COPII following intraluminal injection (ILI) *in vivo*. Distribution of COPI (a) prior to and (b) 15-min post-ILI of Chx266-hGH. Co-localization of COPII (c) prior to and (d) 15-min post-ILI of Chx266-hGH. Arrow = apical epithelial surface; dashed line = epithelial cell-basement membrane demarcation; G = goblet cell; *l-p* = *lamina propria*. Nuclei stained with 4′,6-diamidino-2-phenylindole (DAPI; blue).

(Figure 6d **and line-intensity profile plot**). At 5-min post-ILI, Chx266-hGH also showed significant co-localization with COPII (Figure 6e **and line-intensity profile plot**), but in this case, the extent of COPII co-localizations with Chx266-hGH in the apical vesicular compartment was maintained at 15 min (Figure 6f **and line-intensity profile plot**). Interestingly, Chx266-hGH reaching the basal vesicular compartment at 15 min was sometimes associated with COPII$^+$ vesicles (Figure 6f), but not with COPI$^+$ vesicles (Figure 6d). These results show that the A→B transcytosis of Chx involves sustained interactions with COPII$^+$ vesicles in the apical vesicular compartment, but co-localization with COPI$^+$ vesicles in the supranuclear region that diminishes with time, suggesting that the re-organization of these coating machineries is involved in trafficking mechanisms hijacked by this exotoxin that modify over time.

LMAN1 redistribution is associated with Chx trafficking

The ERGIC is a sorting compartment where COPI$^+$ and COPII$^+$ vesicles intersect.[21] We investigated the role of ERGIC elements in Chx A→B transcytosis by monitoring the distribution of a type I integral membrane protein resident to this vesicular structure that functions as a cargo receptor (ERGIC-53); also known LMAN1 (lectin mannose-binding protein 1).[29] LMAN1 distribution in untreated enterocyte expression was limited to the apical vesicle compartment with a moderate level of co-localizations with COPI$^+$ vesicles (Figure 7a); even fewer co-localization events were observed between LMAN1 and COPII$^+$ vesicles compared to COPI$^+$ vesicles, with the majority of COPII$^+$ vesicles being present near the basal plasma membrane where LMAN1 was not present (Figure 7b). By 15-min post-ILI of Chx266-hGH, COPI$^+$ vesicles were
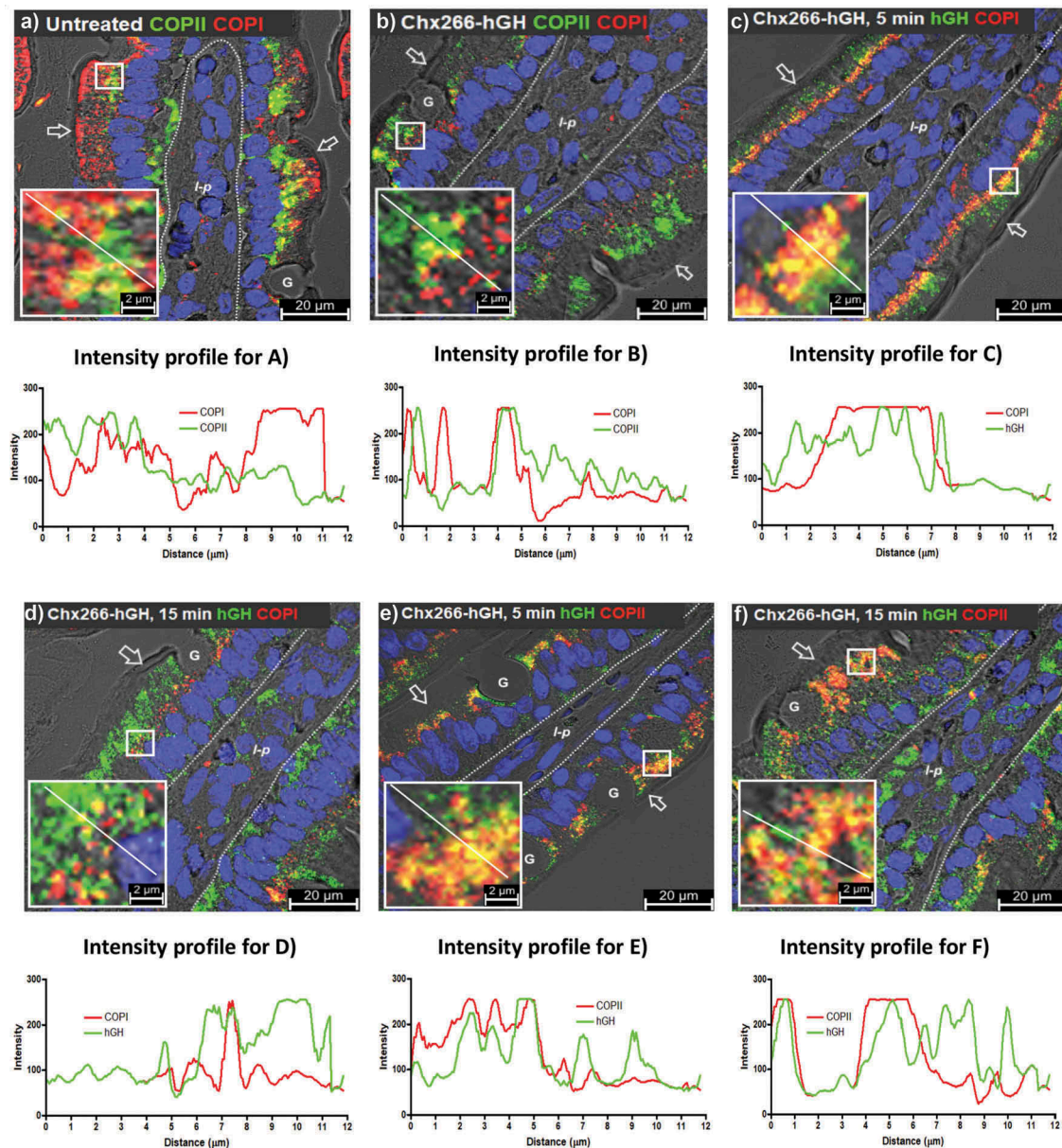
Figure 6. Chx is observed within COPII-positive and COPI-positive vesicles during A→B transcytosis following intraluminal injection (ILI) *in vivo*. Distribution of COPI and COPII (a **and line-intensity profile plot**) prior to and (b **and line-intensity profile plot**) 15-min post-ILI of Chx266-hGH delivered by intraluminal injection into rat jejunum *in vivo*. Co-localization of COPI and Chx266-hGH at 5-min (c **and line-intensity profile plot**) or 15-min (d **and line-intensity profile plot**) post-ILI of Chx266-hGH. Co-localization of COPII and Chx266-hGH at 5-min (e **and line-intensity profile plot**) or at 15-min (f **and line-intensity profile plot**) post-ILI of Chx266-hGH. Arrow = apical epithelial surface; dashed line = epithelial cell-basement membrane demarcation; G = goblet cell; *l-p* = *lamina propria*. Nuclei stained with 4′,6-diamidino-2-phenylindole (DAPI; blue).

restricted to the supranuclear region of enterocytes as previously observed (Figure 5b), while LMAN1 appeared to increase in content and redistribute from an apical-only localization to an apical and basal vesicular compartment distribution, with a discrete set of COPI/LMAN1 co-localizations being observed in the supranuclear region (Figure 7c). At 15-min post-ILI of Chx266-hGH, COPII/LMAN1 co-localizations were observed in the apical vesicular compartment, but not in the basal vesicular compartment following the redistribution of LMAN1 (Figure 7d).

This apparent enhanced expression and redistribution of LMAN1 to the basal vesicular compartment suggested a potential role for this cargo receptor in Chx A→B transcytosis. We tested this possibility in several ways. First, we showed that LMAN1, but not
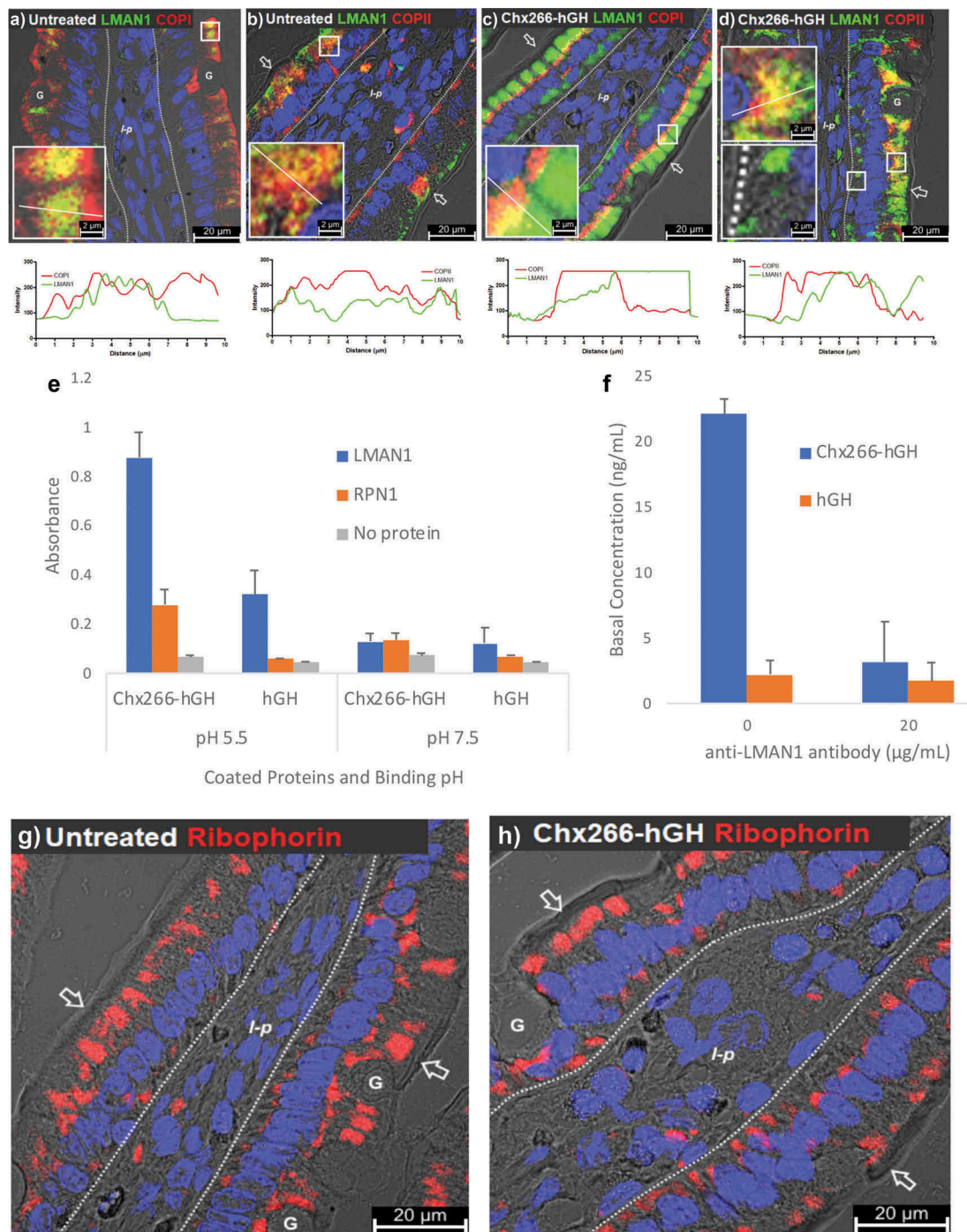
Figure 7. A→B transcytosis of Chx domain I induces a redistribution of LMAN1 following intraluminal injection (ILI) *in vivo*. Co-localization of LMAN1 with (a) COPI or (b) COPII in untreated enterocytes prior to and 15-min post-ILI of Chx266-hGH. Co-localization of LMAN1 with (c) COPI or (d) at 15-min post-ILI. (e) ELISA-based binding interactions between LMAN1 with Chx266-hGH compared to hGH (N = 3; mean ± SE). (f) The extent of *in vitro* A→B transcytosis of Chx266-hGH across SMI-100 tissues after 60 min in the presence and absence of an antibody recognizing LMAN1 (N = 3; mean ± SE). Intracellular localization of Ribophorin in enterocytes (g) before treatment or (h) 15-min post-ILI of Chx266-hGH. Arrow = apical epithelial surface; dashed line = epithelial cell-basement membrane demarcation; G = goblet cell; *l-p* = *lamina propria*. Nuclei stained with 4',6-diamidino-2-phenylindole (DAPI; blue).

a similar type I integral membrane protein found only in the rough endoplasmic reticulum, ribophorin 1 (RPN1), interacted with Chx in an ELISA-type binding assay (Figure 7e). The ERGIC has been identified as the earliest low-pH site in the secretory pathway,[30] and we observed that LMAN1/Chx

interactions were stronger at pH 5.5 compared to pH 7.5 (Figure 7e). Next, we showed that the introduction of an antibody to LMAN1 added to the apical compartment of polarized monolayers of primary human intestinal epithelium dramatically reduced the extent of ntChx undergoing A→B transport *in vitro* (Figure 7f). Finally, we examined the intracellular distribution of RPN1 and found it to have a predominantly apical and basal vesicular compartment distribution (Figure 7g) that was not dramatically altered at 15-min post-ILI of Chx266-hGH (Figure 7h).

LMAN1 redistribution is not associated with ERGIC breakdown

As LMAN1 is regarded as a definitive element of the ERGIC, we investigated the integrity of this compartment following cellular changes associated with Chx-induced LMAN1 reorganization by examining the intracellular distribution of another ERGIC element: SEC22b.[31] In untreated tissues, SEC22b and LMAN1 extensively co-localized in the apical compartment, while LMAN1 alone was separately observed close to the apical plasma membrane (Figure 8a). At 5 min following ILI of Chx266-hGH, LMAN1,

SEC22b, and hGH were observed to co-localize in the apical compartment but not at the apical plasma membrane (Figure 8b). By 10-min post-ILI, hGH and LMAN1 were co-localized in the basal compartment of enterocytes without SEC22b, suggesting that LMAN1 moved with Chx266-hGH from the apical vesicular compartment to basal vesicular compartment in a manner that did not involve a general ERGIC disorganization (Figure 8c). At 15-min post-ILI, the extent of hGH/LMAN1 co-localization in the basal compartment had increased with more hGH reaching the *lamina propria* (Figure 8d). The same tissue sections examined only for LMAN1 and SEC22b (no hGH signal) are shown to highlight LMAN1 redistribution to the basal compartment without a concomitant SEC22b redistribution in response to an apical application of Chx266-hGH (Figure 8e–h).

Chx A→B transcytosis traffics to the basal membrane in a manner similar to HSPG

A→B transcytosis of ntChx was associated with an apical only to apical and basal endosomal compartment reorganization of LMAN1,
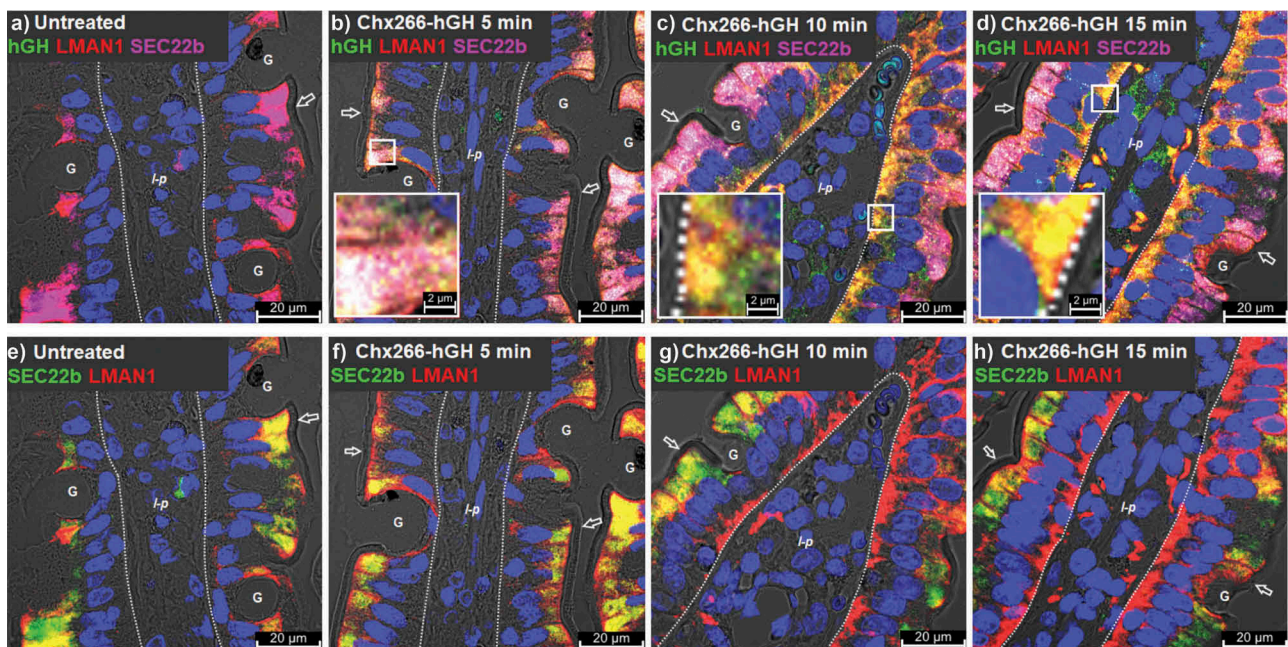
Figure 8. A→B transcytosis for Chx domain I is associated with LMAN1 redistribution but does not affect ERGIC organization. Time-course study of the distribution of (a-d) SEC22b as a marker of ERGIC co-localized with LMAN1 and Chx266-hGH or (e-h) SEC22b and LMAN1 co-localized without showing Chx266-hGH. Arrow = apical epithelial surface; dashed line = epithelial cell-basement membrane demarcation; G = goblet cell; *l-p = lamina propria*. Nuclei stained with 4',6-diamidino-2-phenylindole (DAPI; blue).

suggesting that this pathway involves hijacking an endogenous element for this unexpected routing for a protein entering from the apical enterocyte surface. To further explore this possibility with relation to basal targeting, we examined the distribution of a protein known for its basal secretion from enterocytes: the basement membrane-specific heparan sulfate proteoglycan core protein (HSPG), also known as perlecan. HSPG is a multidomain proteoglycan that binds to and cross-links a variety of extracellular matrix components and cell-surface molecules following its secretion from cells.[32] Importantly, HSPG+ intracellular vesicles have been shown to be enriched in Rab11[33] and ntChx co-localizes with Rab11+ vesicles at the basal membrane of enterocytes (Figure 2d). By 15-min post-ILI, a substantial amount of Chx266-hGH was observed in the basal vesicular compartment of enterocytes that co-localized with LMAN1 and HSPG (Figure 9a–c). In sites adjacent to the basal membrane, hGH was co-localized with LMAN1 (**inset A**), or with HSPG (**inset B**), or both LMAN1 and HSPG (**inset C**). While it is possible that co-localizations of hGH with HSPG could have occurred through endocytosis at the basal plasma membrane, we also observed extensive co-localizations of HSPG with Chx266-hGH in the apical vesicle compartment which coincided with LMAN1 distribution. These data suggest that part of the trafficking strategy used by Chx to achieve A→B transcytosis involves the utilization of vesicular structures that are directed to the basal enterocyte surface with a recycling vesicle signature.[34]

Chx A→B transcytosis can be used for the oral delivery of a biologically active protein cargo

Chx266 was tested for its ability to deliver biologically active hGH following oral gavage. *In vitro* hGH receptor activation studies showed that hGH conjoined to Chx Domain I (Chx266-hGH) was able to induce JAK1 phosphorylation through hGH receptor activation, although at ~3.6-fold less efficient as native hGH based upon calculated EC_{50} values (Figure 10a). At the end of five consecutive days of oral gavage dosing of a liquid formulation of Chx266-hGH in hypophysectomized mice, there was a dose-dependent increase in serum hGH levels (Figure 10b) and a concomitant induction of serum IGF-1 levels (Figure 10c). While these results demonstrate the Chx266 could be used to facilitate the oral delivery of a biologically active cargo, this study was not intended to identify a therapeutic product concept. Importantly, there was no strategy to separate hGH from the Chx266 carrier that would be required for sustained circulating levels of this hormone cargo. Also, despite incorporating a protease inhibitor into the bicarbonate buffer-based formulation to improve the chemical stability of Chx266-hGH prior to intestinal uptake following oral gavage, the amount of intact Chx266-hGH leaving the stomach and reaching the mouse small intestine for trans-epithelial absorption was likely to be extremely limited. Thus, the focus of these studies was to examine the hypothesis that the A→B transcytosis pathway hijacked by Chx did not intersect with cellular degradation elements and could potentially be used for the oral delivery of biopharmaceuticals.
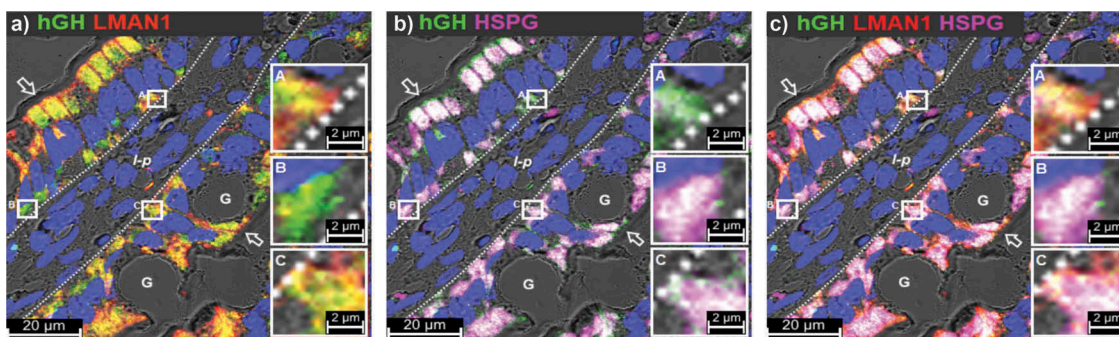

Figure 9. Chx A→B transcytosis involves a basal recycling vesicle compartment. Micrographs represent co-localization of (a) hGH and LMAN1, (b) hGH and HSPG, or (c) hGH, LMAN1, and HSPG at 15-min post-ILI of Chx266-hGH *in vivo* into rat jejunum. Nuclei stained with 4′,6-diamidino-2-phenylindole (DAPI; blue).
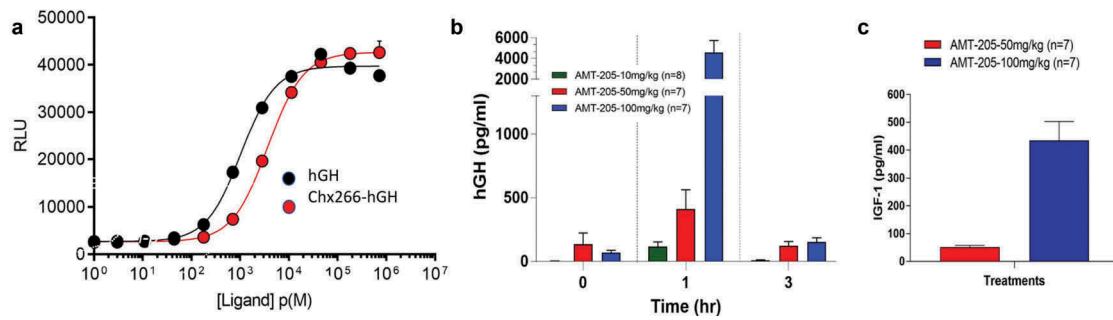
Figure 10. Domain I of Chx can facilitate the oral delivery of biologically active hGH *in vivo*. (a) Receptor activation response curves for hGH and Chx266-hGH show comparable biological activity for hGH following genetic coupling to Chx266 (N = 3; mean ± SE). (b) Serum levels of hGH in hypophysectomized mice at 1 h after the fifth of five consecutive days of oral gavage dosing (N = 7 or 8; mean ± SEM). (c) Serum IGF-1 levels at 3 h after the fifth of five consecutive days of oral gavage dosing (N = 7; mean ± SEM).

Discussion

Overview of pathway strategy used by Chx achieves A→B transcytosis

Chx utilizes a series of intracellular vesicular compartments to traffic through polarized intestinal epithelial cells using a process that culminates in A→B transcytosis. Engagement of clathrin+ vesicles appears to occur in both the apical and basal vesicular compartments, but there is no strong evidence for a clathrin-mediated endocytosis to begin this A→B transcytosis process. The trafficking mechanism used by Chx overcomes endogenous barriers that restrict vesicular movement within cells in order to maintain systemic homeostasis. Cargos within early endosomes, such as those defined by the presence of EEA1 and Rab7, can be sent to the TGN via retrograde trafficking with ultimate targeting to the transitional ER for refolding and repair or sorted to lysosomes for degradation. Importantly, Chx transcytosis uses trafficking elements that avoid delivery to lysosome-like structures. Co-localizations of Chx with TGN-38, however, suggested limited distribution within the TGN during Chx transcytosis. Instead, Chx appears to access the ERGIC element LMAN1 in the apical vesicular compartment soon after endocytosis and uses this interaction to reach the basal vesicular compartment that culminates in basal exocytosis.

LMAN1 functions as a cargo receptor that continuously cycles between the ERGIC and the ER, providing cytoplasmic motifs for recognition by both COPI and COPII components, [21] and functioning in the intracellular transport of a limited set of glycoproteins.[35] Thus, it is possible that the mechanism(s) used by Chx to induce a redistribution of LMAN1 may be also related to the dramatic reorganizations observed for both COPI+ and COPII+ vesicles and intracellular trafficking events critical for a subset of proteins designated for secretion at the basal epithelial plasma membrane. COPI has been described to sort vesicles in both directions through the ER-Golgi systems, with this fate being induced by external cues[36] and COPII is involved in sorting cargos leaving ER exit sites.[37] Due to the COPI and COPII reorganization induced by Chx, it is unclear if these coat proteins remain true to their previously described functions of retrograde and anterograde trafficking. Regardless, this combination of reorganization events is likely the key to how this exotoxin achieves efficient A→B transcytosis. Chx was not associated with the reorganization of other proteins, such as SEC22b and RPN1, affiliated with the cellular location and function of LMAN1, suggesting that the reorganization of both COPI+ and COPII+ vesicles did not effect a gross disruption of vesicular processes in these polarized cells.

A critical aspect of Chx A→B transcytosis involves its capacity to move efficiently from an apical vesicular compartment to a basal vesicular compartment as a prelude to release into the *lamina propria*. Co-localization studies with molecules that are hallmarks of specific intracellular vesicular compartments suggest that Chx transcytosis is not a random process.[38,39] Following apical entry, Chx is observed in an apical vesicular compartment within 1–5 min where it intersects with Rab7 and LAMP1 in a manner that might otherwise signal delivery to lysosomes. By 5–10 min, Chx can be observed in the supranuclear

compartment with the coincident reorganization of an ERGIC element, COPI, and COPII. By 10–15 min, extensive amounts of Chx were observed in a basal vesicular compartment and within the *lamina propria*. This time course, observed *in vivo* in rat small intestine, was consistent with that demonstrated for primary human intestinal epithelium *in vitro*.

Implications for Vibrio cholerae *pathophysiology*

It is notable that both CTx and Chx appear to access host cellular elements that function in directing vesicular contents to retrograde trafficking outcomes that allow these toxins to reach the basal plasma membrane of enterocytes.[40] Unlike CTx, which is secreted by pandemic forms of *V. cholera*, Chx is secreted during nonpandemic infections of this pathogen.[10] Also, while CTx is retained primarily within enterocytes where it induces secretory diarrhea by increasing Cl^- efflux properties of the epithelium,[40] Chx does not appear to intoxicate enterocytes and instead is delivered rapidly to cells within the *lamina propria*. Indeed, a nontoxic form of full-length Chx can transport within 10–15 min across polarized human small intestinal epithelia *in vitro* and rat intestinal epithelia *in vivo*. Further, elements within domain I of Chx that lack the toxic domain III of the protein were shown to be sufficient for transcytosis.

The fact that Chx can rapidly access the intestinal *lamina propria* through a mechanism that does not appear to damage the epithelia suggests a clandestine strategy to stabilize chronic nonpandemic *V. cholerae* infections in the intestinal lumen. Previous studies have suggested that the airway pathogen, *Pseudomonas aeruginosa*, secretes a similar virulence factor (exotoxin A) that also can achieve A→B transcytosis without epithelial cell intoxication.[41] In general, secreted bacterial virulence factors are known for their capacity to produce cellular changes that subvert host cell endocytic and secretory pathway functions.[42] Such cellular changes are commonly observed as a result of infection by obligate and facultative intracellular pathogens, with some pathogens and virulence factors inducing changes in the distribution of intracellular components of polarized intestinal epithelial cells. For example,

Shiga toxin disrupts retrograde vesicle trafficking[43] to incite epithelial cell intoxication.[44] *Vibrio parahaemolyticus* injects a series of virulence factors into enterocytes that alter the polarity properties of these cells as part of their actions to incite seafood-borne gastritis.[45] Our data demonstrate a distinct approach used by an extracellular pathogen to manipulate host cell functions: vesicular trafficking that results in efficient A→B transcytosis of a virulence factor that target cells within the *lamina propria* whose intoxication could limit immune responses and stabilize infections of nonpandemic *V. cholerae* in the intestinal lumen.

Potential applications for A→B transcytosis of biopharmaceuticals

Our observations support the hypothesis that Chx efficiently transports across intact intestinal epithelium through a transcytosis pathway that does not involve enterocyte intoxication or disruption. Such a transcytosis mechanism would predict that intact Chx is delivered to the *lamina propria* where nonpolarized cells could be targeted and intoxicated. Our studies suggest domain I of Chx functions to ferry domains II and III for this intoxication function and we demonstrate that a biopharmaceutical (hGH) can be put in place of these domains to achieve efficient epithelial transcytosis of this protein. Importantly, oral gavage of Chx266-hGH demonstrated dose-dependent pharmacokinetics and the anticipated pharmacodynamics of hGH demonstrated by the induction of serum levels of IGF-1. This initial proof of concept cannot be used to determine *in vivo* bioavailability that might be achieved using a Chx-based epithelial transcytosis as the amount of intact Chx266-hGH leaving the stomach and its access to the luminal epithelial surface of the small intestine following oral gavage is probably low and quite variable. Further, a significant amount of Chx266-hGH that completed epithelial transcytosis would likely be sequestered within the *lamina propria* through uptake by nonpolarized cells that are targeted by this exotoxin. Despite these challenges, it appears that a sufficient amount of Chx266-hGH was able to reach hGH receptors in the liver for IGF-1 induction.

Future applications of Chx as a tool to deliver biopharmaceutical by the oral route appear promising for several reasons. First, non-pandemic forms of *V. cholerae* that secrete Chx are present in the human intestine, suggesting that the transcytosis pathway used by this exotoxin will be clinically relevant. Second, the Chx transcytosis pathway appears to deviate from the typical fate of proteins following apical surface endocytosis into enterocytes: lysosomal destruction. Third, organization of the Chx protein allows for a rather straightforward genetic replacement of its cytotoxic elements with a biopharmaceutical. Fourth, Chx-biopharmaceutical chimeras appear to move as efficiently across intact intestinal epithelia as the native Chx protein. Fifth, as no gross modifications to the intestinal epithelia were induced by Chx transcytosis and repeated oral gavage dosings with Chx266-hGH failed to induce an overt issue of toxicity, Chx-based chimeras appear to provide an efficient format for chronic dosing oral delivery. Thus, the trafficking pathway accessed by Chx can potentially be used for the oral delivery of biologically active protein cargos.

Materials and methods

Expression and purification of ntChx and Chx266-RFP

A nontoxic form of the Chx (ntChx) gene containing the $E^{581}A$ mutation and a C-terminal tag was synthesized by Eurofins Genomics and subcloned into the expression vector pET-26b(+) DNA – Novagen (Millipore; Watford, UK). The tag contained a cysteine, a tobacco Etch Virus (TEV) protease recognition sequence, a second cysteine and hexahistidine (His_6) sequence. The Chx266-RFP gene, containing cholix amino acids 1–266, a polyglycine-serine-threonine amino acid spacer sequence, and red fluorescent protein (RFP) as a cargo, was codon optimized for *E. coli* and synthesized by GenSript USA (Piscataway, NJ, USA). This construct was cloned into the expression vector pET-28a (+) DNA – Novagen (Millipore; Watford, UK) with an N-terminal thrombin-pWETcleavable His_6 tagging sequence. Both the ntChx and Chx266-RFP were expressed in Shuffle T7 Express competent cells (NEB).

Freshly transformed *E. coli* cells were grown at 37°C in Luria Bertani broth (LB), containing kanamycin, to an extinction of 0.6 at 600 nm when the temperature was reduced to 16°C and isopropyl β-D-thiogalactopyranoside (IPTG) was added to a final concentration of 0.5 mM. Growth was continued at 16°C overnight before cells were harvested by centrifugation, resuspended in binding buffer (20 mM histidine pH 8, 300 mM NaCl, 20 mM immidazole) and lysed by sonication. Lysates were centrifuged and supernatant filtered through a 0.45-μm filter. Protein purification was performed using a 5-mL HisTrap™ column (GE Healthcare) connected to an AKTA FLPC. Bound proteins were eluted using a 0.05–1M immidazole gradient and further purified using a Superdex® 200 gel filtration column equilibrated with PBS. Protein purity (>90%) was assessed by SDS-PAGE and protein concentration was assessed using A_{280} prior to storage at −80°C.

Expression and purification of Chx and Chx266-hGH

The Chx266-hGH fusion protein was codon-optimized for E.coli expression and synthesized by GenScript USA, Inc (Piscataway, NJ, USA). The synthesized gene was cloned into the vector pET-26b (+) DNA expression vector and transformed into *E. coli* BL21 (DE3) cells that were cultured by fed-batch fermentation in a 1.8 L stirred tank bioreactor controlled at 30°C, pH 7, in 30% dissolved oxygen on a defined culture media.[46] After 8 h of feeding, cultures were induced with 1-mM IPTG and the temperature was reduced to 26°C. Cultures were continued for a further 12 h after induction before cells were harvested by centrifugation. *E. coli* cell pellets were suspended in 0.5 M NaCl and lysed using high-pressure homogenization with a Microfluidizer LM10 (Microfluidics Corporation, Westwood, MA) at 18,000 PSI. Lysates were clarified by centrifugation for 1 h at 18,600 x*g*, with pellets washed twice with water to isolate insoluble protein inclusion bodies that were then solubilized in 8 M guanidine HCl and clarified using centrifugation at 75,000 x*g* for 1 h. Solubilized inclusion bodies were diluted in refolding buffer (50 mM Tris buffer pH8, 0.5 M L-arginine, 2 M Urea, 1.5 M guanidine, 2 mM $CaCl_2$, 2 mM $MgCl_2$, 0.3 mM glutathione disulfide,

1mM glutathione, and 20mM DTT) at a protein concentration of 0.2 g/L and gently mixed overnight to allow protein refolding. After buffer exchange into 25 mM Tris pH 8, 100 mM urea, and 100 mM NaCl using dialysis and filtration with 0.2-µm membrane, the protein was captured on a Q Sepharose® Fast Flow and isolated by increasing the NaCl gradient from 0 to 0.5 M at pH 8.0 over 24-column volumes. A polishing step using a 40-µm ceramic hydroxyapatite (CHT) Type I column and an increasing linear phosphate gradient from 0.01 to 0.12 M over 10-column volumes was used to achieve further purification. Final protein concentration was assessed using A_{280}, endotoxin was measured using Charles River Endosafe PTS reader, and purity (>90%) was assessed using SDS-PAGE as well as SE-HPLC.

Western blotting

Samples were separated by electrophoresis in a 4–12% NuPAGE gel (BioRad) prior to transfer onto a PVDF membrane (BioRad). Bands positive for Chx elements were labeled using an anti-Chx rabbit polyclonal antibody (prepared in house at AMT) and detected using an alkaline phosphatase (AP)-conjugated secondary goat anti-rabbit antibody (1:10000, Abcam, Cambridge, MA, USA). Protein bands were visualized using an AP Western blotting substrate (Promega, Madison, WI, USA).

ELISA

ntChx-biotin. 96-well Costar plates (Corning, Corning Life Sciences B.V., Amsterdam, The Netherlands) were coated with streptavidin (Rockland, Limerick, PA) for capture ntChx-biotin. After blocking with 3% BSA, samples were added, following dilution into 3% BSA, to wells and incubated for 1 h at RT. Captured ntChx-biotin was detected using the anti-Chx rabbit pAb (prepared in house at AMT). *Chx266-hGH and hGH.* 96-well Costar plates (Corning) were coated with a Chx rabbit polyclonal antibody (prepared in house at AMT). After blocking with 3% BSA, samples were added, following dilution into 3% BSA, to wells and incubated for 1 h at RT. Chx266-hGH was detected using an anti-hGH mAb (R&D systems). A commercial hGH ELISA

kit (R&D Systems) was used to quantitate hGH. Absorbance values for the enzymatic reactions at 405 nm were registered in an ELISA microplate reader (Bio-Rad). *Interactions between ntChx and LMAN1 or RPN1.* 96-well plates were coated with Chx266-hGH or an equal molar concentration of hGH (to serve as a control) in PBS. Wells were blocked in 3% BSA. Flag-tag-labeled versions of LMAN1 or RPN1 (Origene Technologies, Inc., Rockville, MD) at 2 µg/ml in 3% BSA (pH 5.5 or pH 7.5) were then incubated for 1 h at RT. Wells coated with 3% BSA without proteins served as an additional control. The captured LMAN1 or RPN1 were detected using anti-Flag mAb (Origene Technologies, Inc). All ELISA plates were run in triplicate.

In vitro transport

Confluent monolayers of human small intestinal tissues (SMI-100, MatTek Corporation; Ashland, MA, USA) established on cell culture inserts were allowed to stabilize for 24 h at 37°C prior to use. Only inserts having a transepithelial electric resistance (TEER) of >400 $\Omega \bullet cm^2$ were considered to have sufficient monolayer integrity for use in studies. A secondary verification of monolayer integrity was performed by assessing suppression 70-kD dextran transport with detectable levels of transport after 15 min demonstrating defective barrier function. Monolayers were washed once with transport buffer (PBS) before test molecules, prepared at a concentration of 20 µg/mL, were applied to the apical surface in 100-µL volumes. Basolateral volumes of 500-µL PBS were replaced at each time point for transport studies. Each experimental condition was performed in triplicate.

In vivo transcytosis

Male Wistar rats, housed 3–5 per cage with a 12/12 h light/dark cycle, were 225–275 g (approximately 6–8 weeks old) when placed on study. All experiments were conducted during the light phase using a nonrecovery protocol that used continuous isoflurane anesthesia. A 4–5 cm midline abdominal incision exposed mid-jejunum regions. Stock solutions of test articles prepared at 3.86×10^{-5} M were prepared in phosphate-buffered saline (PBS) and administered by

intraluminal injection (ILI) in a 50-µL volume using a 29-gauge needle. The mesentery adjacent to the ILI site was denoted with using a permanent marker. At study termination, a 3–5 mm region that captured the marked intestine segment was isolated and processed for microscopic assessment. All experiments were performed in accordance with the U.K. Animals Scientific Procedures Act of 1986, the European Communities Council Directive of 1986 (86/609/EEC), and the University of Bath's ethical review procedures.

Immunofluorescence microscopy

Isolated intestinal tissues were fixed in 4% paraformaldehyde for 18 h at 4°C, processed using a Leica TP1020 tissue processor, dehydrated in increasing concentrations of ethanol, cleared with HistoClear (National Diagnostics), and infused with molten paraffin wax. Sections cut from tissue-embedded paraffin wax blocks (5-µm thickness; Jung Biocut2035 microtome) were mounted on glass microscope slides, rehydrated, and processed for antigen retrieval by boiling slides in 10-mM sodium citrate for 10 min. Processed tissue slices were permeabilized using 0.1% Triton X-100 in PBS for 30 min, blocked using 2% donkey serum and 2% BSA in 0.1% Triton X-100 in PBS for 2 h, and incubated overnight at 4°C with primary antibodies diluted in 1% BSA and 0.05% Triton X-100 in PBS at 4°C. Tissue slices were washed thrice with PBS, incubated for 2 h with secondary antibodies conjugated to AlexaFluor® fluorescent dyes, washed thrice with PBS, and incubated for 1 h with 200-nM DAPI, washed with PBS, dehydrated in ethanol, and covered by mounting a coverslip with Fluorshield (Abcam) mounting media; all steps performed at room temperature. After allowing the mounting media to dry at 4°C overnight, fluorescent images were obtained using a Zeiss 880 LSM confocal microscope using the following settings. For Alexafluor 488 the excitation wavelength was 488 nm and the emission wavelength was 562 nm. The pinhole was set to 1.01 airy units (AU) to achieve a z-resolution of 0.8 µm. For Alexafluor 564 the excitation wavelength was 561 nm and the emission wavelength was 602 nm. The pinhole was set to 0.99 AU to achieve a z-resolution of 0.8 µm. For Alexafluor 633 the excitation wavelength was 633 nm and the emission wavelength was 693 nm. The pinhole was set to 0.83 AU to achieve

a z-resolution of 0.8 µm. For DAPI the excitation wavelength was 405 nm and the emission wavelength was 462 nm. The pinhole was set to 1.22 (AU) to achieve a z-resolution of 0.8 µm. All laser intensities were set at 2%. All images were captured with a total magnification of x630. Post capture intensity plot analysis was carried out using Zeiss Zen 2.6 Blue software.

Characterization of human growth hormone bioactivity

Human growth hormone (hGH) and Chx266-hGH were evaluated for their capacity to activate the hGH receptor using the PathHunter® eXpress GHR-JAK2 functional assay (Eurofins 93-0829E3CP14M). This assay uses a cell line engineered to co-express a ProLink™ (PK) tagged cytokine receptor, an untagged cytosolic tyrosine kinase, and an enzyme acceptor (EA) tagged SH2 domain where receptor phosphorylation leads to SH2-EA recruitment and forced complementation of the two β-galactosidase enzyme fragments (EA and PK).

Oral gavage studies

Hypophysectomized male C57/BL6 mice (The Jackson Laboratory, Sacramento, CA, USA) were obtained at 15-16-week-old of age (~22 g) and maintained on normal mouse chow and allowed to acclimate for 7 days prior to placement onto study. Chx266-hGH was prepared in 0.2 M sodium bicarbonate buffer (pH 8.5) containing 10 mg/mL soybean trypsin inhibitor and dosed by oral gavage at either 10, 50, or 100 mg/kg, providing an equivalent dose of ~3.3, ~17, and ~33 mg/kg hGH exposure. Nonfasted mice were dosed (200 µL) for five consecutive days with serum samples collected at 1 and 3 h following the fifth and final dosing.

Materials

Primary antibodies: Goat anti-human growth hormone pAb; R&D systems (AF1067); rabbit anti-cholix antiserum; mouse anti-EEA1 mAb; Abcam (ab70521); mouse anti-LAMP1 mAb; Abcam (ab25630); mouse anti-Rab7 mAb; Santa Cruz Biotechnology (sc-376362); mouse anti-Rab11a

mAb; Santa Cruz Biotechnology (sc-166912), mouse anti-TGN38 mAb; Novus (NB300-575); mouse anti-Clathrin mAb; Abcam (ab2731); mouse anti-Calnexin mAb: Santa Cruz Biotechnology (sc-23954). *Secondary antibodies*: Donkey anti-mouse IgG-alexafluor647; Invitrogen (A31571); donkey anti-rabbit IgG-alexafluor546; Invitrogen (A10040); donkey anti-goat IgG-alexafluor488; Invitrogen (A11055).

Highlights

The cholix (Chx) exotoxin protein secreted by *Vibrio cholerae* can efficiently undergo apical to basal (A→B) transcytosis across intact polarized intestinal epithelia.

This A→B transcytosis process utilizes a vesicular trafficking mechanism does not involve the cell intoxication function associated with this exotoxin.

Chx domain I is sufficient for A→B transcytosis, providing a platform to ferry a covalently associated therapeutic protein cargos across the intestinal epithelium.

A→B transcytosis of Chx domain I avoids the lysosomal degradation pathway and results in the oral delivery of a biologically active cargo.

Acknowledgments

Author contributions

Design and preparation of constructs: Julia MacKay, Floriane Laurent, Tom Hunter, Khushdeep Mangat, Lisa Song, Elbert Seto, Sally Postlethwaite, Aatif Alam, Weijun Feng

In vitro studies: Keyi Liu

In vivo studies: Alisatair Taverner, Apurva Chandalia, Minji Seung, and Mazi Saberi

Study concept and writing of manuscript: Randall J. Mrsny.

Declaration of interests

Tom Hunter, Khushdeep Mangat, Lisa Song, Elbert Seto, Sally Postlethwaite, Aatif Alam, Weijun Feng, Keyi Liu, Apurva Chandalia, Minji Seung, and Mazi Saberi are employees/shareholders of Applied Molecular Transport. Randall J. Mrsny is a founder of Applied Molecular Transport and a member of its scientific advisory board.

Disclosure of potential conflicts of interest

No potential conflicts of interest were disclosed.

Funding

ORCID

Alistair Taverner http://orcid.org/0000-0002-2507-8694
Randall J. Mrsny http://orcid.org/0000-0001-8505-8516

References

1. Schneeberger K, Roth S, Nieuwenhuis EES, Middendorp S. Intestinal epithelial cell polarity defects in disease: lessons from microvillus inclusion disease. Dis Model Mech. 2018;11(2):dmm031088. doi:10.1242/dmm.031088.

2. Nelson WJ. Remodeling epithelial cell organization: transitions between front-rear and apical-basal polarity. Cold Spring Harb Perspect Biol. 2009;1(1):a000513. doi:10.1101/cshperspect.a000513.

3. Ruch TR, Engel JN. Targeting the mucosal barrier: how pathogens modulate the cellular polarity network. Cold Spring Harb Perspect Biol. 2017;9(6):a027953. doi:10.1101/cshperspect.a027953.

4. Pott J, Hornef M. Innate immune signalling at the intestinal epithelium in homeostasis and disease. EMBO Rep. 2012;13(8):684–698. doi:10.1038/embor.2012.96.

5. Ahmed W, Zheng K, Liu ZF. Establishment of chronic infection: Brucella's stealth strategy. Front Cell Infect Microbiol. 2016;6:30. doi:10.3389/fcimb.2016.00030.

6. Faruque SM, Mekalanos JJ. Pathogenicity islands and phages in Vibrio cholerae evolution. Trends Microbiol. 2003;11(11):505–510. doi:10.1016/j.tim.2003.09.003.

7. Gorbach SL, Banwell JG, Pierce NF, Chatterjee BD, Mitra RC. Intestinal microflora in a chronic carrier of Vibrio cholerae. J Infect Dis. 1970;121(4):383–390. doi:10.1093/infdis/121.4.383.

8. Chen Y, Johnson JA, Pusch GD, Morris JG Jr., Stine OC. The genome of non-O1 Vibrio cholerae NRT36S demonstrates the presence of pathogenic mechanisms that are distinct from those of O1 Vibrio cholerae. Infect Immun. 2007;75(5):2645–2647. doi:10.1128/IAI.01317-06.

9. Faruque SM, Chowdhury N, Kamruzzaman M, Dziejman M, Rahman MH, Sack DA, Nair GB, Mekalanos JJ. Genetic diversity and virulence potential of environmental Vibrio cholerae population in a cholera-endemic area. Proc Natl Acad Sci U S A. 2004;101(7):2123–2128. doi:10.1073/pnas.0308485100.

10. Purdy AE, Balch D, Lizarraga-Partida ML, Islam MS, Martinez-Urtaza J, Huq A, Colwell RR, Bartlett DH. Diversity and distribution of cholix toxin, a novel ADP-ribosylating factor from Vibrio cholerae. Environ Microbiol Rep. 2010;2(1):198–207. doi:10.1111/j.1758-2229.2010.00139.x.

11. Jorgensen R, Purdy AE, Fieldhouse RJ, Kimber MS, Bartlett DH, Merrill AR. Cholix toxin, a novel ADP-ribosylating factor from Vibrio cholerae. J Biol Chem. 2008;283(16):10671–10678. doi:10.1074/jbc.M710008200.

12. Lugo MR, Merrill AR, Father T. Son and cholix toxin: the third member of the DT Group Mono-ADP-Ribosyltransferase toxin family. Toxins (Basel). 2015;7(8):2757–2772. doi:10.3390/toxins7082757.

13. Fieldhouse RJ, Jorgensen R, Lugo MR, Merrill AR. The 1.8 A cholix toxin crystal structure in complex with NAD+ and evidence for a new kinetic model. J Biol Chem. 2012;287(25):21176–21188. doi:10.1074/jbc.M111.337311.

14. FitzGerald D, Mrsny RJ. New approaches to antigen delivery. Crit Rev Ther Drug Carrier Syst. 2000;17(3):165–248. doi:10.1615/CritRevTherDrugCarrierSyst.v17.i3.

15. Watson P, Spooner RA. Toxin entry and trafficking in mammalian cells. Adv Drug Deliv Rev. 2006;58(15):1581–1596. doi:10.1016/j.addr.2006.09.016.

16. Melby EL, Jacobsen J, Olsnes S, Sandvig K. Entry of protein toxins in polarized epithelial cells. Cancer Res. 1993;53:1755–1760.

17. Tyagi P, Pechenov S, Anand Subramony J. Oral peptide delivery: translational challenges due to physiological effects. J Control Release. 2018;287:167–176. doi:10.1016/j.jconrel.2018.08.032.

18. Smith DC, Spooner RA, Watson PD, Murray JL, Hodge TW, Amessou M, Johannes L, Lord JM, Roberts LM. Internalized Pseudomonas exotoxin A can exploit multiple pathways to reach the endoplasmic reticulum. Traffic. 2006;7(4):379–393. doi:10.1111/j.1600-0854.2006.00391.x.

19. Spooner RA, Smith DC, Easton AJ, Roberts LM, Lord JM. Retrograde transport pathways utilised by viruses and protein toxins. Virol J. 2006;3:26. doi:10.1186/1743-422X-3-26.

20. Guo Y, Sirkis DW, Schekman R. Protein sorting at the trans-Golgi network. Annu Rev Cell Dev Biol. 2014;30:169–206. doi:10.1146/annurev-cellbio-100913-013012.

21. Szul T, Sztul E. COPII and COPI traffic at the ER-Golgi interface. Physiology (Bethesda). 2011;26(5):348–364. doi:10.1152/physiol.00017.2011.

22. Jerdeva GV, Tesar DB, Huey-Tubman KE, Ladinsky MS, Fraser SE, Bjorkman PJ. Comparison of FcRn- and pIgR-mediated transport in MDCK cells by fluorescence confocal microscopy. Traffic. 2010;11(9):1205–1220. doi:10.1111/j.1600-0854.2010.01083.x.

23. Bucci C, Thomsen P, Nicoziani P, McCarthy J and van Deurs B. Rab7: a key to lysosome biogenesis. Mol Biol Cell. 2000;11(2):467–480. doi:10.1091/mbc.11.2.467.

24. Mateus D, Marini ES, Progida C, Bakke O. Rab7a modulates ER stress and ER morphology. Biochim Biophys Acta Mol Cell Res. 2018;1865(5):781–793. doi:10.1016/j.bbamcr.2018.02.011.

25. Modica G, Skorobogata O, Sauvageau E, Vissa A, Yip CM, Kim PK, Wurtele H, Lefrancois S. Rab7 palmitoylation is required for efficient endosome-to-TGN trafficking. J Cell Sci. 2017;130(15):2579–2590. doi:10.1242/jcs.199729.

26. Zhang S, Zheng H, Chen Q, Chen Y, Wang S, Lu L, Zhang S. The lectin chaperone calnexin is involved in the endoplasmic reticulum stress response by regulating Ca 2+ homeostasis in aspergillus nidulans. Appl Environ Microbiol. 2017;83(15). doi:10.1128/AEM.00673-17.

27. Subach FV, Verkhusha VV. Chromophore transformations in red fluorescent proteins. Chem Rev. 2012;112(7):4308–4327. doi:10.1021/cr2001965.

28. Cullen PJ, Steinberg F. To degrade or not to degrade: mechanisms and significance of endocytic recycling. Nat Rev Mol Cell Biol. 2018;19(11):679–696. doi:10.1038/s41580-018-0053-7.

29. Zhu M, Zheng C, Wei W, Everett L, Ginsburg D, Zhang B. Analysis of MCFD2- and LMAN1-deficient mice demonstrates distinct functions in vivo. Blood Adv. 2018;2(9):1014–1021. doi:10.1182/bloodadvances.2018018317.

30. Appenzeller-Herzog C, Hauri HP. The ER-Golgi intermediate compartment (ERGIC): in search of its identity and function. J Cell Sci. 2006;119(Pt 11):2173–2183. doi:10.1242/jcs.03019.

31. Cebrian I, Visentin G, Blanchard N, Jouve M, Bobard A, Moita C, Enninga J, Moita L, Amigorena S, Savina A, et al. Sec22b regulates phagosomal maturation and antigen crosspresentation by dendritic cells. Cell. 2011;147(6):1355–1368. doi:10.1016/j.cell.2011.11.021.

32. Gubbiotti MA, Neill T, Iozzo RV. A current view of perlecan in physiology and pathology: A mosaic of functions. Matrix Biol. 2017;57–58:285–298. doi:10.1016/j.matbio.2016.09.003.

33. Podyma-Inoue KA, Moriwaki T, Rajapakshe AR, Terasawa K, Hara-Yokoyama M. Characterization of heparan sulfate proteoglycan-positive recycling endosomes isolated from glioma cells. Cancer Genomics Proteomics. 2016;13(6):443–452. doi:10.21873/cgp.20007.

34. van Ijzendoorn SC. Recycling endosomes. J Cell Sci. 2006;119(Pt 9):1679–1681. doi:10.1242/jcs.02948.

35. Vollenweider F, Kappeler F, Itin C, Hauri HP. Mistargeting of the lectin ERGIC-53 to the endoplasmic reticulum of HeLa cells impairs the secretion of a lysosomal enzyme. J Cell Biol. 1998;142(2):377–389. doi:10.1083/jcb.142.2.377.

36. Park SY, Yang JS, Schmider AB, Soberman RJ, Hsu VW. Coordinated regulation of bidirectional

COPI transport at the Golgi by CDC42. Nature. 2015;521(7553):529–532. doi:10.1038/nature14457.

37. Nie C, Wang H, Wang R, Ginsburg D, Chen XW. Dimeric sorting code for concentrative cargo selection by the COPII coat. Proc Natl Acad Sci U S A. 2018;115 (14):E3155–E62. doi:10.1073/pnas.1704639115.

38. Apodaca G, Gallo LI, Bryant DM. Role of membrane traffic in the generation of epithelial cell asymmetry. Nat Cell Biol. 2012;14(12):1235–1243. doi:10.1038/ncb2635.

39. Stenmark H. Rab GTPases as coordinators of vesicle traffic. Nat Rev Mol Cell Biol. 2009;10(8):513–525. doi:10.1038/nrm2728.

40. Lencer WI, Tsai B. The intracellular voyage of cholera toxin: going retro. Trends Biochem Sci. 2003;28 (12):639–645. doi:10.1016/j.tibs.2003.10.002.

41. Mrsny RJ, Daugherty AL, McKee ML, FitzGerald DJ. Bacterial toxins as tools for mucosal vaccination. Drug Discov Today. 2002;7(4):247–258. doi:10.1016/S1359-6446(01)02139-0.

42. Weber MM, Faris R. Subversion of the endocytic and secretory pathways by bacterial effector proteins. Front Cell Dev Biol. 2018;6:1. doi:10.3389/fcell.2018.00001.

43. Hall G, Kurosawa S, Stearns-Kurosawa DJ. Shiga toxin therapeutics: beyond neutralization. Toxins (Basel). 2017;9(9):291–309.

44. Park JY, Jeong YJ, Park SK, Yoon SJ, Choi S, Jeong DG, Chung S, Lee B, Kim J, Tesh V, et al. Shiga toxins induce apoptosis and ER stress in human retinal pigment epithelial cells. Toxins (Basel). 2017;9(10):319. doi:10.3390/toxins9100319.

45. O'Boyle N, Boyd A. Manipulation of intestinal epithelial cell function by the cell contact-dependent type III secretion systems of Vibrio parahaemolyticus. Front Cell Infect Microbiol. 2014;3:114.

46. Korz DJ, Rinas U, Hellmuth K, Sanders EA, Deckwer WD. Simple fed-batch technique for high cell density cultivation of Escherichia coli. J Biotechnol. 1995;39(1):59–65. doi:10.1016/0168-1656(94)00143-Z.